ISIJ International, Vol. 58 (2018), No. 1, pp. 98–106

Effect of Super-gravity Field on Grain Refinement and Tensile Properties of Cu–Sn Alloys

Yuhou YANG,[1,2] Bo SONG,[1,2]* Jin CHENG,[2] Gaoyang SONG,[1,2] Zhanbing YANG[1,2] and Zeyun CAI[1,2]

1) State Key Laboratory of Advanced Metallurgy, University of Science and Technology Beijing, Beijing, 100083 China.
2) School of Metallurgical and Ecological Engineering, University of Science and Technology Beijing, Beijing, 100083 China.

(*Received on May 3, 2017; accepted on August 29, 2017; J-STAGE Advance published date: October 6, 2017*)

In this paper, the effect of super-gravity field on the grain refinement and tensile properties of as-cast Cu–Sn alloys were investigated systematically. The experimental results revealed that the as-cast grains of Cu–Sn alloys can be significantly refined in super-gravity field. In normal gravity field, the average grain size is 2.13 mm, while in super-gravity fields of G=100, 300 and 600, they are 0.35 mm, 0.173 mm and 0.074 mm, respectively. Accordingly, both the tensile strength and the plasticity are enhanced with the increasing gravity coefficient. The ultimate tensile strength of Cu-11wt%Sn sample in normal gravity field is 265 MPa, while in super-gravity fields of G=100, 300 and 600, they are 449 MPa, 487 MPa and 521 MPa, respectively. The fracture morphology transforms from fragility to plasticity with the increasing gravity coefficient. The mechanism for the grain refinement is that super-gravity promotes the falling of crystal nuclei within the solidifying melt only at the early solidification period, which can be called the "Crystal Rain". As a result, the crystal nuclei multiply within the solidifying melt and a refined grain structure was obtained. Besides, the refining effect by super-gravity increases with the increasing solute Sn concentration because of the increased nucleation rates and a decrease in crystal growth.

KEY WORDS: super-gravity field; grain refinement; tensile properties; Cu–Sn alloys.

1. Introduction

It is well known that the mechanical properties of castings can be improved by grain refinement. Common methods to refine the grain structure are adding grain refiner into the melt and low temperature casting in the casting process.[1)] With the development of external physical field technology, many articles have been published concerning the magnetic, electric current and ultrasonic fields on the grain refinement.[2–7)] However, super-gravity is often overlooked in regards to the effects of external physical fields on the solidification structure.

In recent years, super-gravity technology exhibited great advantages on the metal purification and the recovery of valuable metals.[8–13)] In the field of casting, metallurgists were mainly focused on the mold filling behavior by centrifugal method previously.[14–17)] However, studies specialized to grain refinement of castings in super-gravity field are seldom reported as a whole and the refining mechanism is far from clear.

Previously, four mechanisms were contributed to the structure refinement of as-cast alloys under super-gravity (centrifugal force) field: the change of nucleation energy mechanism by Chen *et al.*,[18)] the dendrite fragments mechanism by Zhao *et al.*,[19)] the coexist of free-chill crystals and the dendrite fragments mechanism by Chang *et al.*,[20)] and the faster cooling mechanism by Wu *et al.*[21)] Thereinto, the change of nucleation energy is qualitative rather than quantitate. Thus, to what extent that the solidification structure can be refined is not clear by the change of nucleation energy under elevated gravity. However, Zhao *et al.* hold the opposite opinion with Chen, but his dendrite fragments mechanism lacks sufficient proof. Chang's mechanism seemed more reasonable, but a detailed explanation for the crystals' moving behavior was not presented. Wu's simulation study did not take account of the movement of equiaxed grains, which can markedly influence the solidification structure of castings.[22,23)] Also, the solidification structure refinement of Al–Cu alloys in super-gravity field has been investigated systematically in our recent study,[24)] which demonstrated that the "crystal rain" caused by super-gravity contributed to the grain refinement.

For the limitation that super-gravity technology has restrict demand for the experimental apparatus, previous researches related to structure refinement in super-gravity (centrifugal force) field are mainly conducted with aluminum alloys, which have a low melting temperature. In addition, the subsequent mechanical properties of the castings were not payed attention. Therefore, based on our early research, the grain refinement of higher-melting temperature metals by super-gravity and simultaneously the mechanical properties deserve to be explored.

In the present article, the effect of super-gravity field on

* Corresponding author: E-mail: songbo@metall.ustb.edu.cn
DOI: http://dx.doi.org/10.2355/isijinternational.ISIJINT-2017-233

the grain refinement and tensile properties of Cu–Sn alloys was investigated with different gravity coefficients and solute contents. Furthermore, by applying super-gravity field at different solidification stages of Cu-11wt%Sn alloy, the refining mechanism was revealed experimentally and discussed combined with the density variations of solid and remaining liquid.

2. Experimental

2.1. Super-gravity Apparatus

In this research, super-gravity apparatus consists of two furnaces that revolves around a rotation axis as outlined in the schematic **Fig. 1**.[9] The real size of the apparatus is approximately L×W×H= 900 mm×1 000 mm×1 300 mm. A program controller and an R type thermocouple were used to control the temperature within ± 3 K. Before each experiment, we firstly adjust the apparatus to balance carefully. When the apparatus is in rotation state, it could generate a vibration with a low frequency which is almost equal to the rotation frequency.

The gravity coefficient that evaluates the super-gravity field is calculated as the ratio of super-gravitational acceleration to the normal- gravitational acceleration via Eq. (1).[13]

$$G = \sqrt{g^2 + (\omega^2 r)^2} \Big/ g = \sqrt{g^2 + \left(\frac{N^2 \pi^2 r}{900}\right)^2} \Big/ g \quad \text{..... (1)}$$

Where, G is the gravity coefficient, ω is the angular velocity (rad/s), N is the rotation speed (r/minute), r is the distance between the centrifugal axis and the sample (0.25 m), g is the normal-gravitational acceleration (9.8 m/s^2).

2.2. Materials Preparation

The Cu–Sn alloys were prepared with pure Cu (99.99 wt%) and pure Sn (99.99 wt%). Pure Cu and specific mass of pure Sn were put into an alumina crucible. Then they were placed in a molybdenum wire furnace to be heated to 1 423 K with argon gas (99.99%) protection at a flowrate of 0.5 L/min and held at temperature for 1 hour. During holding, the melt was stirred three times to keep a uniform composition. After that, the molten metal was water quenched to acquire the base metal for super-gravity experiments.

The covering slag was a mixture of 45 wt% sodium chloride and 55 wt% potassium chloride to protect the samples from oxidation during the experiments.

2.3. Super-gravity Experimental Procedures

In the super-gravity experiments, the base metal (115 g) and covering slag (10 g) were put into an alumina crucible (inner diameter 20 mm) and then they were heated to 1 423 K in the super-gravity heating furnace. After holding the temperature at 1 423 K for 10 minutes, the melt temperature was controlled to decrease at a decreasing rate of 10 K/min. The super-gravity apparatus was started when the temperature fell to the liquidus temperature. The apparatus was kept under operation until the temperature fell to the specific temperature, which is 50 K lower than the solidus to assure a completely solid sample, after which the super-gravity apparatus was shut off and the sample was water quenched immediately to keep its as-cast structure. At the same time,

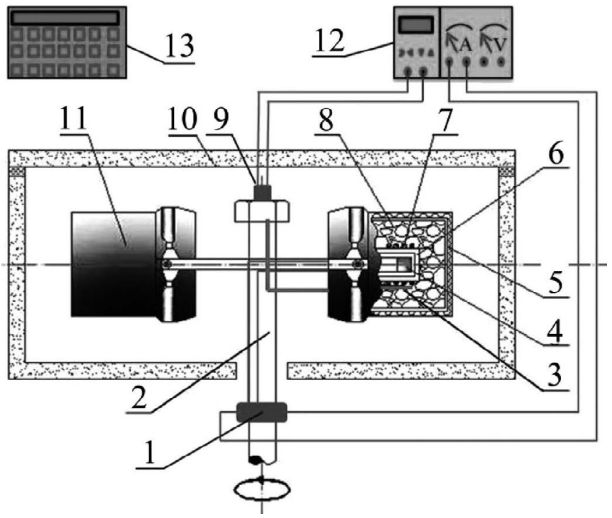

Fig. 1. Schematic diagram of super-gravity apparatus:[9] 1, conductive slip ring; 2, rotation axis; 3, thermocouple; 4, sample; 5, furnace shell; 6, furnace tube; 7, resistance wire; 8, thermal insulation materials; 9, thermocouple conductive slip ring; 10, housing; 11, counterpart; 12, temperature controller; 13, rotation controller.

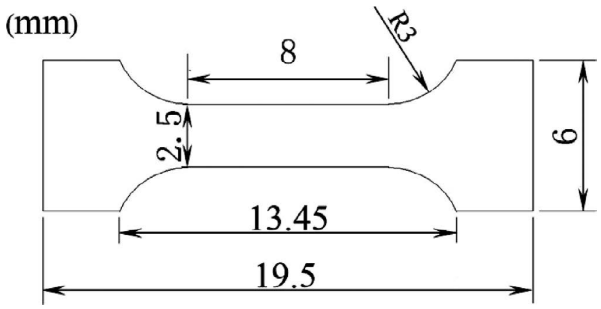

Fig. 2. Schematic geometry of tensile testing specimen.

we also obtained one sample in normal gravity field under the same cooling rate, which was as the parallel sample.

The samples obtained were central cut longitudinally into two halves, one of which was grinded, polished and etched with a mixture of 5 g $FeCl_3$: 50 ml hydrochloric acid: 100 ml water to reveal the grain structure. The macro- and micro-structure were examined by a digital camera and a metallurgical microscope (9XB-PC type), respectively. The grain size is measured by liner intercept method.

In order to study the effects of super-gravity field on tensile properties of as-cast Cu-11wt%Sn alloy, tensile tests were performed using an electronic universal testing machine (CTM8000) with the strain rate of 1.71×10^{-4}/s at room temperature. **Figure 2** shows the testing specimen with 2 mm thickness. All the specimens were obtained at the center of the as-cast sample. Then the fracture morphology was observed under a scanning electron microscope (SEM-EDS, MLA250, FEI).

3. Results and Discussion

3.1. Macro- and Micro-structures of As-cast Cu-11wt%Sn Samples in Normal Gravity and Super-gravity Field

The macro-structure of as-cast Cu-11wt%Sn samples obtained with different gravity fields at cooling rate of 10

K/min is shown in **Fig. 3**. As there is friction force at the connecting axle, the furnace cannot be completely horizontal in the rotation state, which results in the skewed free surface at the top of samples. When G=1 (normal gravity field), the solidification structure is mainly coarse bulk crystals as exhibited in Fig. 3(a). While in super-gravity field of G=100 as shown in Fig. 3(b), the grain size decreased obviously compared with that in normal gravity field. When gravity coefficient increased up to 300 and 600, most area of the longitudinal section were occupied by extremely fine grains as shown in Figs. 3(c) and 3(d), especially for the sample with the gravity coefficient of G=600, illustrating that super-gravity can greatly refine the solidification structure of as-cast Cu-11wt%Sn alloy.

Figure 4 depicts the microstructure at the center region of the as-cast Cu-11wt%Sn sample. In normal gravity field, the crystals are so developed dendritic morphology that a dendrite cannot be fully included in a picture at the magnification of 100× as shown in Fig. 4(a). When gravity coefficient increases to 100, both the primary and the secondary dendrite size decrease apparently as shown in Fig. 4(b), indicating a microstructure transition from columnar dendrite to equiaxed dendrite. When gravity coefficient increases to 300, the dendrites have transformed into globular grains with legible grain boundary as shown in Fig. 4(c). When gravity coefficient is up to 600, the grain size is further decreased and the microstructure consists of mainly fine equiaxed grains as shown in Fig. 4(d). On the whole, the dendrite size decreases and the structure transforms into equiaxed grains with increasing the gravity coefficient.

Figure 5 summarizes the average grain size of the samples obtained in normal gravity field and super-gravity field. It can be seen that when in normal gravity field, the average grain size is 2.13 mm, and it is 0.35 mm when gravity coefficient increases to G=100. The grain size is only 74 μm when gravity coefficient is up to 600. As a whole, the aver-

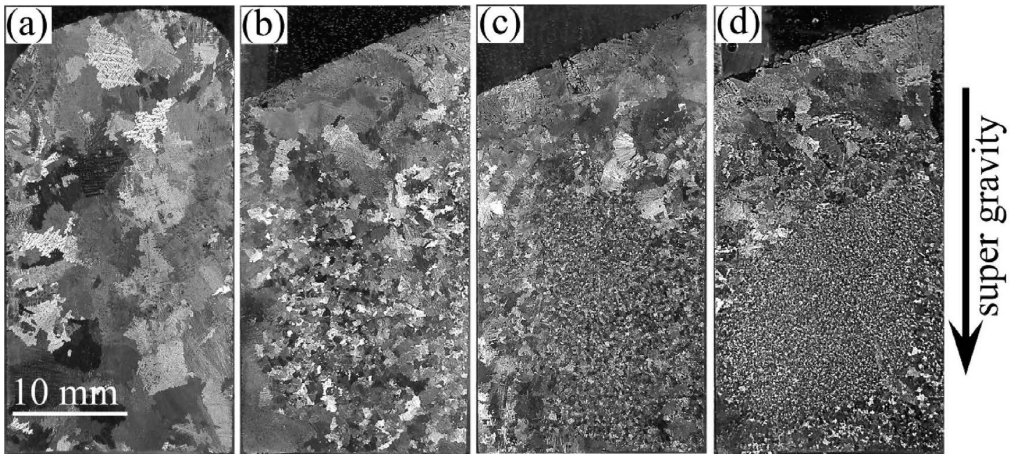

Fig. 3. Macro-structure of as-cast Cu-11wt%Sn samples obtained in normal gravity and super-gravity fields: (a) G = 1, (b) G = 100, (c) G = 300, (d) G = 600.

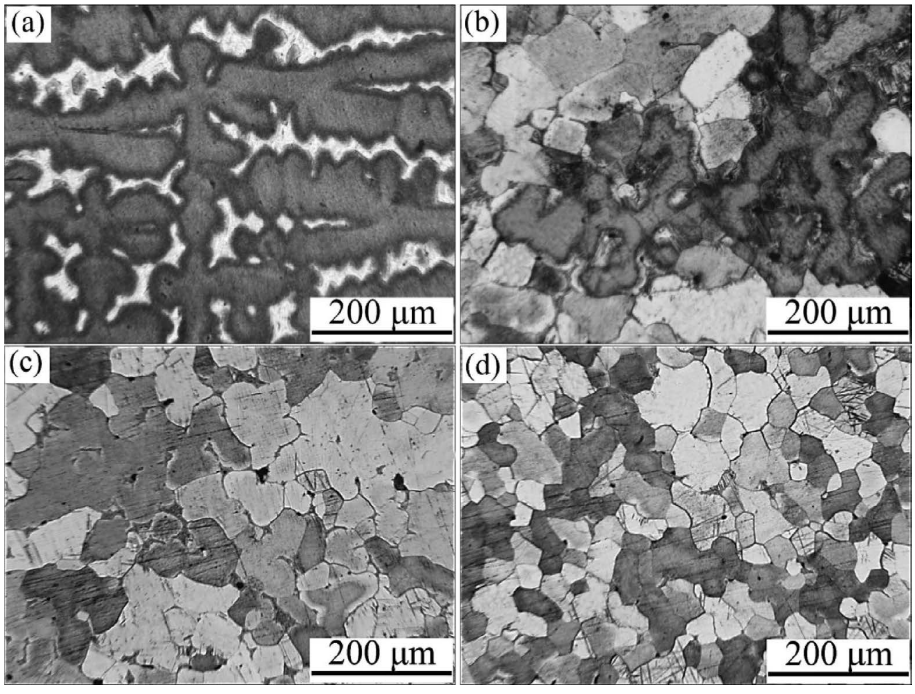

Fig. 4. Micro-structure at the center region of as-cast Cu-11wt%Sn samples in normal gravity and super-gravity fields: (a) G = 1, (b) G = 100, (c) G = 300, (d) G = 600.

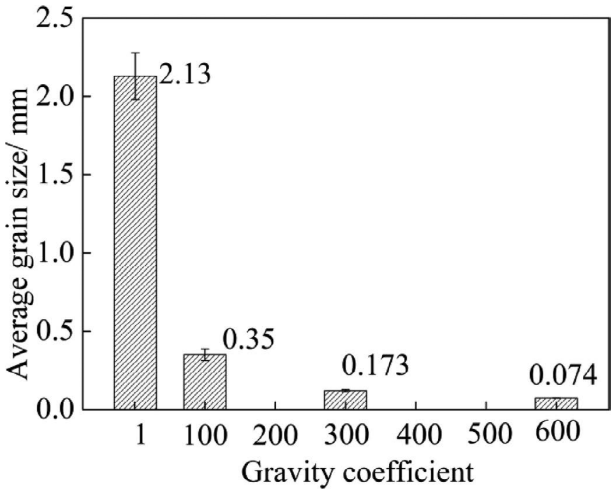

Fig. 5. Average grain size of as-cast Cu-11wt%Sn samples in normal gravity and super-gravity fields.

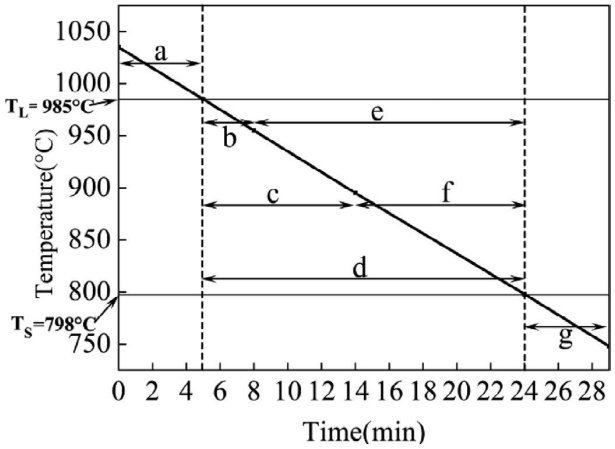

Fig. 6. Schematic diagram of super-gravity G=300 application at different solidifying stages of Cu-11wt%Sn alloy.

age grain size decreases with the increasing gravity coefficient, which agrees with the macro- and micro-structures in Figs. 3 and 4. This also illustrates that super-gravity can markedly refine the grain structure of Cu-11wt%Sn alloys.

Aiming at exploring the mechanism for the grain refinement of Cu-11wt%Sn alloy in super-gravity field, experiments were conducted by applying super-gravity of G=300 at different solidifying stages as shown in **Fig. 6**. The (a) stage and (g) stage correspond to liquid and solid stages, respectively. The (b), (c) and (d) stages correspond to the period that the solid fraction increases from 0 to 20%, 50% and 100%, respectively. The (e) and (f) stages correspond to the period that the solid fraction increases from 20% and 50%, respectively, to 100%.

It can be observed from **Figs. 7**(a) and 7(g) that when super-gravity field was applied at the completely liquid stage and the completely solid stage, both the as-cast structures exhibit coarse bulk and columnar grains, approximately the same as that without super-gravity treatment. This illustrates that the grain structure can neither be refined by applying super-gravity field at the completely liquid stage nor after the end of solidification.

When super-gravity field was applied at (b)–(d) stages in Fig. 6, all the as-cast structures are very fine grains and the grains becomes slightly refined with the prolonging treatment as shown in Fig. 7(b) through Fig. 7(d). This illustrates that much refined grains can be obtained with just applying super-gravity treatment at the early solidification period of the Cu-11wt%Sn alloy.

When super-gravity field was applied at (e)–(f) stages in Fig. 6, it can be found from Figs. 7(e) and 7(f) that fine grains can be always obtained as long as super-gravity treatment was included at the first half of solidification stage. But the structure is still coarse bulk grains, the same as that without super-gravity treatment when just applying super-gravity at the second half of solidification process as shown in Fig. 7(f). This illustrates that it is of no sense to the grain refinement with super-gravity treatment at the second half of solidification stage.

Figure 8 summarizes the average grain size of Cu-11wt%Sn samples obtained by applying super-gravity field at different solidifying stages marked in Fig. 6. It can be seen that the average grain size is as large as 2.08 mm and 2.26 mm for samples with applying super-gravity field at the liquid and solid stages, respectively, which is consistent with the macrostructures in Figs. 7(a) and 7(g). While the grain size decreases to only 0.274 mm in super-gravity field of G=300 and the grain size decreases with prolonging the treatment, which is in agreement with Fig. 7(a) through Fig. 7(d). The grain size is still as small as 0.226 mm when super-gravity was applied during the solid fraction of 0.2 to 1, illustrating that the grain structure can be always refined as long as super-gravity was included at the first half of solidification stage. However, when super-gravity was only applied at the second half of solidifying stage, the grain size is as large as 2.11 mm, which is almost the same without super-gravity treatment.

Gong *et al.* and Liao *et al.* studied the solidification structure refinement of pure Al by electric pulse magneto-oscillation and current pulse,[25,26] and they proved that the falling of crystal nuclei, namely the "Crystal Rain" contributed to the refining mechanism. It is only at the early solidification stage that the main refining effect can be obtained in their work, which is also similar with the present experimental results. Considering the fact that the most remarkable characteristic is that super-gravity can significantly promote the relative motion between solid-liquid, gas-liquid and liquid-liquid because of the difference in density.[27–33] What's more, our previous study[24] reported that the "crystal rain" caused by super-gravity was contributed to the mechanism of the grain refinement of Al–Cu alloys. Therefore, it is expected that a similar mechanism is occurring in super-gravity field as a result of the moving behavior of crystal nuclei.

At the present cooling condition (ν = 10 K/min), the densities of the precipitated solid and the remaining liquid are always changing during the coexistence in the whole solidification process. The calculated density variations of both solid and the remaining liquid of Cu-11wt%Sn alloy is displayed in **Fig. 9**. We can know from the result that the crystal's density is always higher than the liquid's density. Prior to solidification, the density of the liquid increases with the decreasing temperature, which fits with the common rule that the density of metals increases with the decreasing temperature. However, due to the small partition coefficient of Cu–Sn alloy,[34] the solute Sn with a smaller

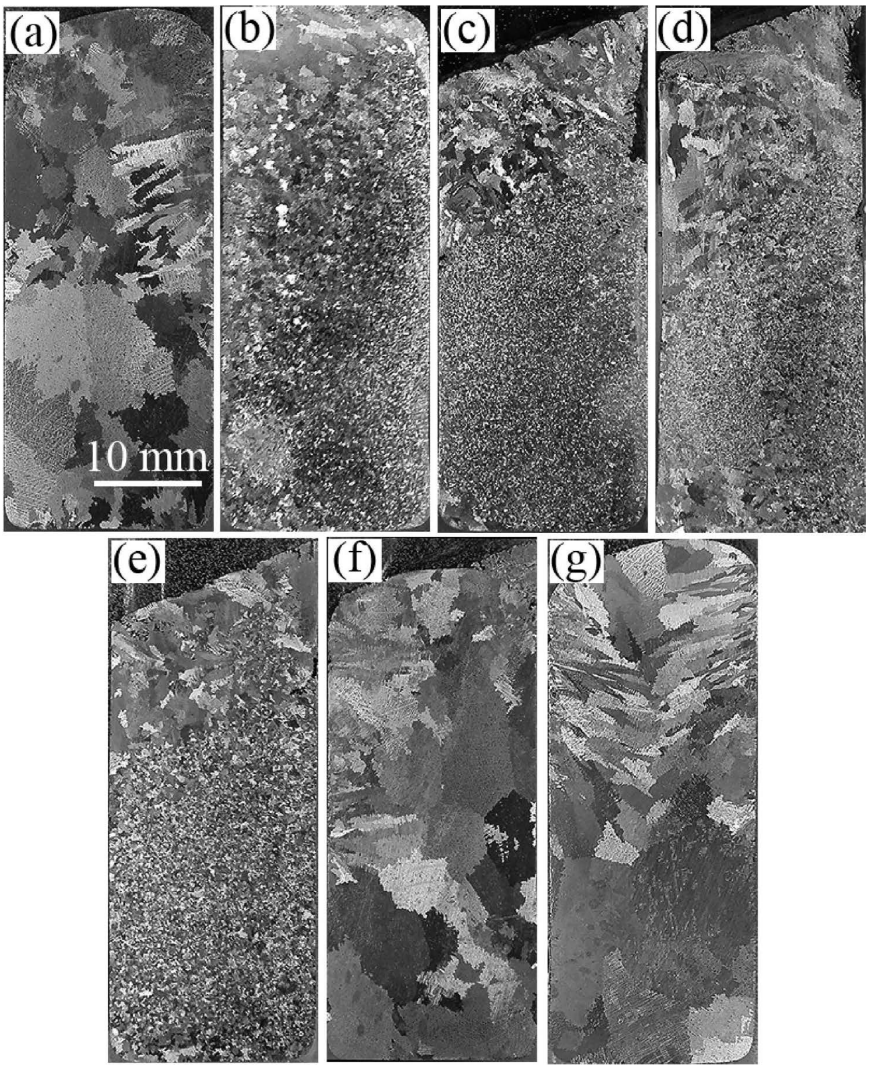

Fig. 7. Macro-structure of as-cast Cu-11wt%Sn samples of applying super-gravity field of G=300 at different solidifying stages marked in Fig. 6: (a): liquid stage, (b): 0–20%, (c): 0–50%, (d): 0–100%, (e): 20%–100%, (f): 50%–100%, (g): solid stage.

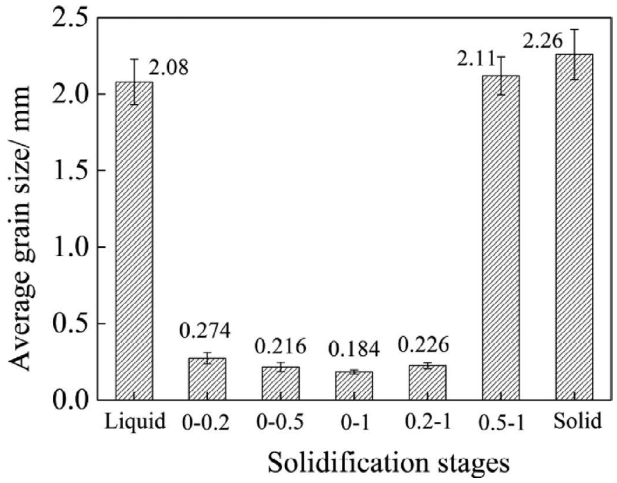

Fig. 8. The average grain size of Cu-11wt% samples with applying super gravity of G=300 at different solidifying stages marked in Fig. 6.

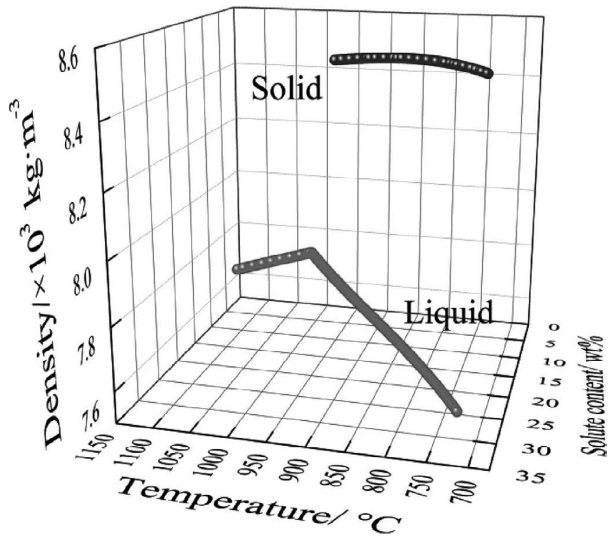

Fig. 9. Density change of solid and remaining liquid of Cu-11wt%Sn alloy in the solidifying process calculated via Jmatpro7.0 software.

density (ρ_{Sn} = 7 300 kg/m^3) than that of Cu (ρ_{Cu} = 8 900 kg/m^3) is rapidly enriched in the remaining liquid. As a result, the liquid's density starts to decrease gradually after solidification proceeds.[35] While the density of the crystals increases slightly with the decreasing temperature.

A solid particle's moving velocity in the liquid can be understood through Stokes' law[36,37] as follows:

$$\frac{\pi}{6}d^3(\rho_l-\rho_p)Gg-3\pi\eta d\frac{dr}{dt}=\frac{\pi}{6}d^3\rho_p\frac{d^2r}{dt^2} \quad \text{..... (2)}$$

Where d is the diameter of the solid particle (m), ρ_p and ρ_l are the densities of the solid particle and the liquid (kg/m^3), η is the viscosity of the liquid (Pa s), r is the displacement of the solid particle (m).

Then the moving velocity of particles in equilibrium can be presented as follows:

$$V_r=d^2(\rho_l-\rho_p)Gg/18\eta \quad \text{..... (3)}$$

In normal gravity field, considering the fact that the viscosity of the molten metal is generally large, for example the viscosity of liquid copper is approximately 4.5 mPa s at 1 373 K,[38,39] which is 4.5 times as large as that of water at 293 K (1 mPa s),[40] and the crystal nuclei is very small in size, the crystal nuclei can hardly move during solidification. Besides, the primary α-Cu crystals are usually dendrite-form, which increase the moving resistance a lot.[41] Therefore, crystal sedimentation can hardly happen in normal gravity field though the solid's density is larger than the liquid's density. However, under the effect of super-gravity, the falling velocity of crystals is much intensified and then large amount of crystal nuclei falls down, generating the "Crystal Rain" and thus leading to the multiplication of grains in the solidifying melt. As a result, very fine grains of Cu-11wt%Sn sample is obtained by applying super-gravity. As more crystal nuclei were generated in super-gravity field, the dendrite arms cannot grow up. Finally, the microstructure transformed from coarse dendrite to fine globular grains as shown in Fig. 4.

Since the tube is heat insulated all around except the top, the temperature at the top surface of the sample should be the lowest in the cooling process. So the earliest nuclei were formed at the upper surface. Then super gravity promoted the settle down of the nuclei. In addition, the crucible wall was also the nucleation site and the crystals nucleated on the crucible wall would also fall down under the super gravity.

The crystals could move freely only at the early solidification stage, but at the second half of the solidification stage, the solid fraction is so large that the dendrites connect with each other into network and the crystals could not move freely anymore.[35] On the other hand, Fleming's experimental results indicated that the apparent viscosity increased dramatically when the solid fraction reached about 40 wt% in his research concerning with the behavior of metal alloys in the semisolid state.[42] Based on the above points, the "Crystal Rain" can only happen at the early solidification period. Therefore, only applying super-gravity at the early solidification can greatly refine the grain structure of Cu-11wt%Sn alloy and it is of no sense by applying super-gravity at the second half of solidification process as demonstrated in Figs. 7(b) and 7(f).

In addition, K. Kocatepe *et al.* reported the "Effect of low frequency vibration on macro and micro structures of LM6 alloys".[43] They found that vibration frequency at 15 Hz and 21.7 Hz did not give an appreciable reduction in grain size but a significant decrease in grain size took place when the vibration frequency was increased to between 31.7 and 41.7 Hz and to amplitudes between 0.375 and 0.5 mm. F. Taghavi *et al.* also reported that mechanical vibration with a frequency of 10 Hz had little effect on the grain size and morphology of A356 aluminum alloy and prolonging the vibration time is of no good at this frequency. When the frequency increased to 30 Hz, the grain size decreased obviously.[44,45] With regard to our research, the super gravity were G=100, 300 and 600, corresponding to the rotation speed of 600 r/min, 1 039 r/min and 1 460 r/min. So the vibration frequency is approximately 10 Hz, 17.3 Hz and 24.3 Hz, which were rather low frequency. Therefore, according to the above-mentioned references, the vibration caused by the rotation of the apparatus cannot generate significant influence on the solidification structure. In addition, the super gravity, which is hundreds of times larger than the normal gravity, is so large that refined structure is mainly caused by super gravity.

3.2. Macro-structures of As-cast Cu–Sn Samples with Different Solute Sn Concentrations in Normal Gravity Field and Super-gravity Field

With the purpose of studying the influence of solute concentration on the grain refinement by super-gravity field, experiments were conducted on Cu–Sn alloys containing four varying solute Sn concentrations (the weight pct of Sn were 0, 2, 6, and 11, respectively). **Figure 10** exhibits the macro-structures of the resulting samples obtained in normal gravity field and super-gravity field at cooling rate of v = 10 K min^{-1}. As can be seen in Fig. 10(a), when G = 1 and wt%Sn=0, few clear grains morphology is observed since the grain size of pure Cu is too large and the sample is too small in size with a diameter of only 19 mm. When G = 1 and the Sn concentration increases to 2 wt%, grain morphology appears but it is extremely coarse as shown in Fig. 10(b). The structure is gradually refined but still remains to be coarse bulk grains with further increasing Sn concentration as shown in Figs. 10(c) and 10(d). The variety of the grains in normal gravity field indicates that although the grains is gradually refined with increasing solute Sn concentration, the grains still remain coarse bulk morphology and cannot transform into fine equiaxed grains. While in super-gravity field with G = 600 as shown in Fig. 10(e), the solidification structure of pure Cu becomes coarse equiaxed grains with legible grain boundary, which is much finer than that in normal gravity field. However, when the Sn concentration is 2 wt%, many finer grains appear though some bulk crystals still remain as shown in Fig. 10(f). When the Sn concentration increases to 6 wt%, the structure is mainly fine grains as shown in Fig. 10(g). The grains is further refined when the Sn concentration is up to 11 wt% as shown in Fig. 10(h). The evolution of grain structures illustrates that in super-gravity field, the grain refining effect can be markedly enhanced by the increasing solute Sn concentration.

The average grain size of Cu–Sn samples containing varying solute Sn concentrations is summarized is **Fig. 11**. The grain size is not provided for pure Cu sample in normal gravity field due to the invisible of grain morphology. The grain size for all the Cu–Sn samples in super-gravity field is much smaller than that in normal gravity field. Furthermore, the refining effect by super-gravity is greatly enhanced with the increasing solute content, which agrees well with the macro-structures in Fig. 10.

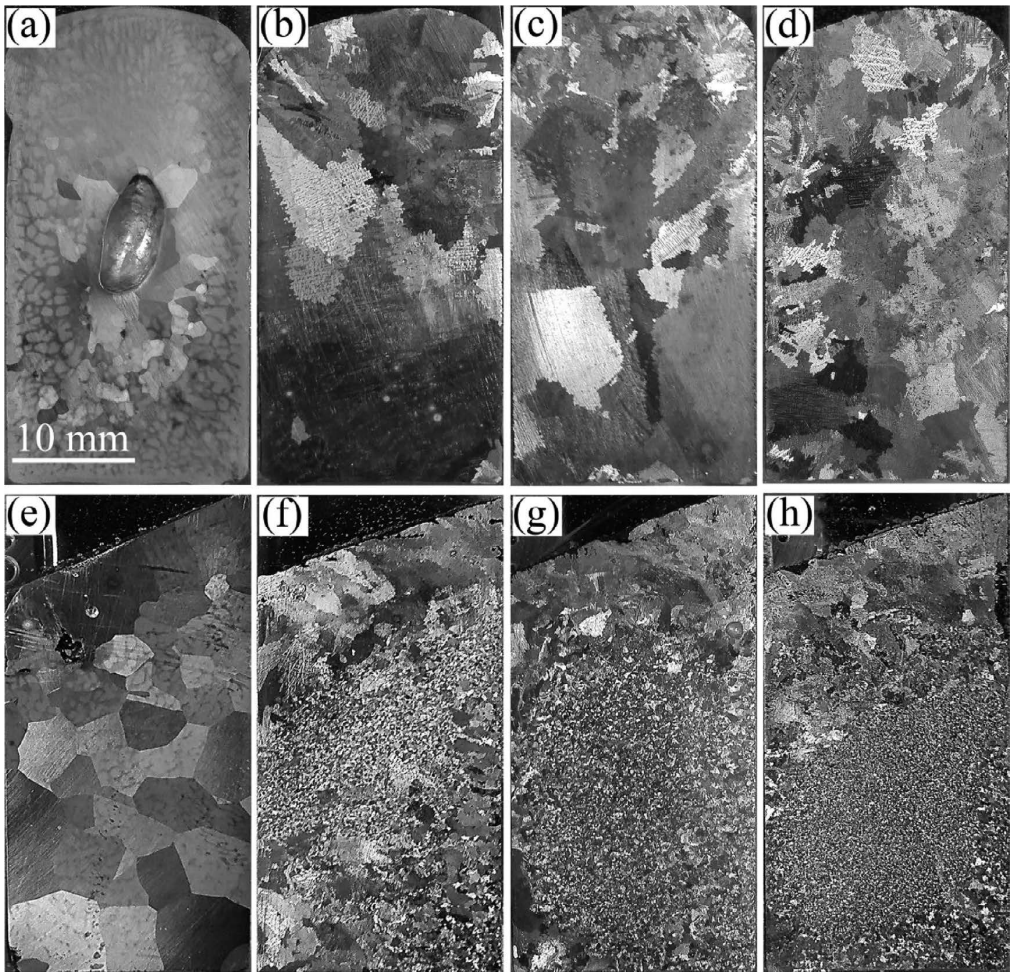

Fig. 10. Macro-structures of Cu–Sn samples containing varying solute Sn concentrations in normal gravity field and super-gravity field: (a) G = 1, 0 wt%Sn, (b) G = 1, 2 wt%Sn, (c) G = 1, 6 wt%Sn, (d) G = 1, 11 wt%Sn, (e) G = 600, 0 wt%Sn, (f) G = 600, 2 wt%Sn, (g) G = 600, 6 wt%Sn (h) G = 600, 11 wt%Sn.

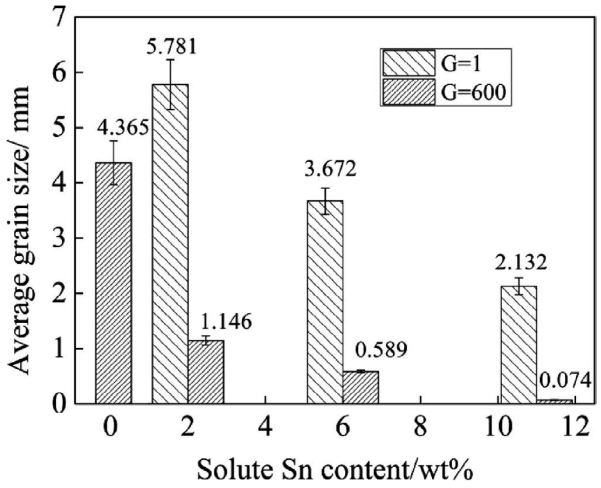

Fig. 11. Average grain size of Cu–Sn samples with varying solute content obtained in normal gravity field and super gravity field of G = 600.

Since the grain structure of as-cast Cu–Sn alloys can be only refined by applying super-gravity field at the early solidification period, the grain refinement is closely related to the nucleation rate of Cu–Sn alloys containing varying solute Sn concentrations.[46] Further, during their falling process under the effect of super-gravity, the crystals keep growing up, which directly influences the crystals size and then affects the moving velocity. Thus, the grain refinement is also influenced by the growth velocity of the primary α-Cu crystals. Chang *et al.*[20] found that the Al alloys were more refined with the increasing solute Si concentration in centrifugal casting process. They also pointed out that under any conditions, more concentrated alloys had a larger nucleation rate than alloys containing less solute, and the dendrite grew much faster for alloys containing less solute. Previous literatures[47,48] also reported that solute element could restrict the growing of crystals. Consequently, for Cu–Sn alloys containing more solute Sn, not only more nuclei could form, but also the nuclei grew slower than alloys containing less solute Sn, both of which can lead to a heavier "Crystal Rain" in super-gravity field. Therefore, it is well explained why the grain structure is more refined with increasing solute Sn concentration in super-gravity field.

In addition, according to Stokes' law, the moving velocity is in direct proportion to the density contrast. For the present Cu–Sn alloys, at the initial solidification, the density contrast between the solid and remaining liquid increases with increasing solute Sn concentration as pointed in **Fig. 12** calculated via Jmatpro7.0 software. Hence, increasing the solute Sn concentration also helps for the falling down of crystals based on this analysis and thereby promoting a larger "Crystal Rain" in super-gravity field.

3.3. Tensile Properties of As-cast Cu-11wt%Sn Samples in Normal Gravity and Super-gravity Fields

The stress-strain curves at room temperature for the as-cast Cu-11wt%Sn samples are shown in **Fig. 13**. It is clear that the stress-strain curves become taller and broader with the increasing gravity coefficient, illustrating that both the strength and plasticity increase. When in normal gravity field, the ultimate tensile strength value is only 265 MPa, while in super-gravity field of G = 100, the ultimate strength increases to 449 MPa. When gravity coefficient increases to 600, the strength is up to 521 MPa.

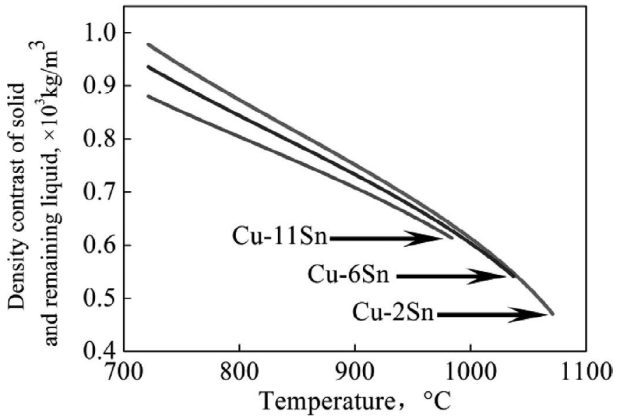

Fig. 12. The density contrast of solid and remaining liquid in the solidifying Cu–Sn alloys calculated via Jmatpro7.0 software.

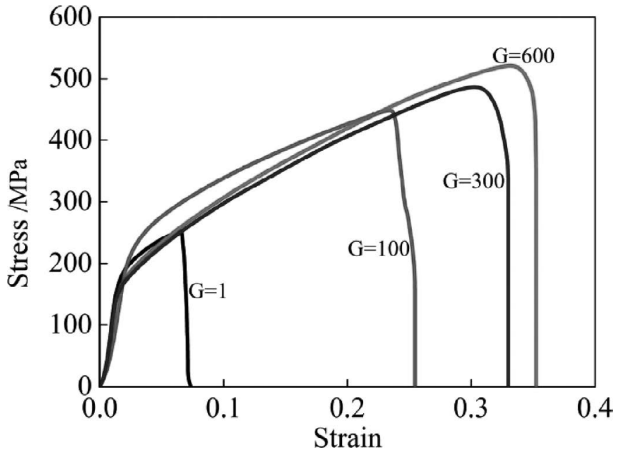

Fig. 13. Stress-strain curves of Cu-11wt%Sn samples in normal gravity and super-gravity fields.

Figure 14 shows the fracture morphology in the center region of as-cast Cu-11wt%Sn samples after tensile tests. In normal gravity field, the fracture exhibits developed dendritic morphology, which is the intergranular brittle fracture, while in super-gravity field of G = 100, instead of dendritic morphology, a few dimples begin to appear, and when gravity coefficient increases to 300 and 600, the fractures contain a large amount of dimples, indicating a transformation from friability to plasticity.

It is well-known that the decrease in grain size can increase both the strength and the plasticity.[49,50] In the present study, the grain size decreases with the increasing gravity coefficient as clearly shown in Figs. 3 and 4, as a result of which, both the strength and plasticity are enhanced remarkably. Therefore, it is well demonstrated that super-gravity can effectively enhance both the strength and plasticity of the as-cast Cu-11wt%Sn alloy through decreasing the grain size. Besides, the variety in fracture morphology is in agreement with the stress-strain curves and the improvement in plasticity can be also confirmed by the large amount of dimples in the fracture morphology in Fig. 14.

4. Conclusions

The grain refinement and tensile properties of as-cast Cu–Sn alloys in super-gravity field were investigated. The conclusions drawn are as follows:

(1) The as-cast grains of Cu–Sn alloys can be significantly refined in super-gravity field.

(2) The grain refining mechanism of as-cast Cu–Sn alloys in super-gravity field is that super-gravity extremely

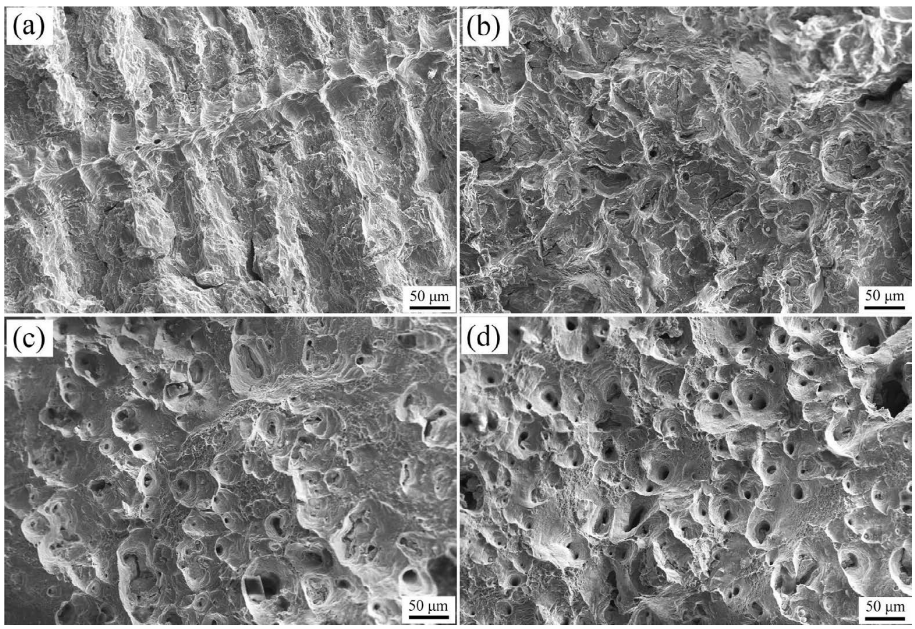

Fig. 14. The fracture morphology at the center region of as-cast Cu-11wt%Sn samples in normal gravity and super-gravity fields: (a) G = 1, (b) G = 100, (c) G = 300, (d) G = 600.

intensifies the falling of crystal nuclei only at the early solidification stage, promoting the grain multiplication and causing the solidification structure refinement finally. Increasing the solute Sn concentration can increase the nucleation rate and slow the growth of solidifying grains, which help develop grain refinement in super-gravity field.

(3) Super-gravity can greatly enhance the tensile properties of as-cast Cu-11wt%Sn alloy through decreasing the grain size. Both the tensile strength and plasticity are greatly enhanced with the increasing gravity coefficient and the fracture exhibits a transformation from fragility to plasticity.

Acknowledgement

This work is financially supported by the National Natural Science Foundation of China (Nos. 51234001 and 51274269). The authors would like to sincerely thank the State Key Laboratory of Advanced Metallurgy, University of Science and Technology Beijing for using the super-gravity apparatus.

REFERENCES

1) A. Radjai and K. Miwa: *Metall. Mater. Trans. A*, **33** (2002), 3025.
2) J. Li, J. H. Ma, Y. L. Gao and Q. J. Zhai: *Mater. Sci. Eng. A*, **490** (2008), 452.
3) J. H. Ma, L. Li, Y. L. Gao and Q. J. Zhai: *Mater. Lett.*, **63** (2009), 142.
4) A. Radjai and K. Miwa: *Metall. Mater. Trans. A*, **31** (2000), 755.
5) X. Jian, H. Xu, T. T Meek and Q. Han: *Mater. Lett.*, **59** (2005), 190.
6) Y. Cui, C. L. Xu and Q. Han: *Scr. Mater.*, **55** (2006), 975.
7) X. Jian, T. T. Meek and Q. Han: *Scr. Mater.*, **54** (2006), 893.
8) G. Y. Song, B. Song, Y. H. Yang, Z. B. Yang and W. B. Xin: *Metall. Mater. Trans. B*, **46** (2015), 2190.
9) Y. H. Yang, B. Song, G. Y. Song, Z. B. Yang and W. B. Xin: *Metall. Mater. Trans. B*, **47** (2016), 2714.
10) J. C. Li, Z. C. Guo and J. T. Gao: *ISIJ Int.*, **54** (2014), 743.
11) J. T. Gao, L. Guo and Z. C. Guo: *ISIJ Int.*, **55** (2015), 2535.
12) F. Q. Wang, J. T. Gao, X. Lan and Z. C. Guo: *ISIJ Int.*, **57** (2017), 200.
13) J. T. Gao, Y. W. Zhong and Z. C. Guo: *ISIJ Int.*, **56** (2016), 1352.
14) K. Watanabe, O. Miyakawa, Y. Takada, O. Okuno and T. Okabe: *Biomaterials*, **24** (2003), 1737.
15) G. Chirita, D. Soares and F. S. Silva: *Mater. Des.*, **29** (2008), 20.
16) K. Liu, Y. C. Ma, M. Gao, G. B. Rao, Y. Y. Li, K. Wei, X. H. Wu and M. H. Loretto: *Intermetallics*, **13** (2005), 925.
17) J. Bohacek, A. Kharicha, A. Ludwig and M. H. Wu: *ISIJ Int.*, **54** (2014), 266.
18) K. Y. Chen, Z. Q. Hu and B. Z. Ding: *J. Mater. Sci. Technol.*, **10** (1994), 307.
19) L. X. Zhao, Z. C. Guo, Z. Wang and M. Y. Wang: *Metall. Mater. Trans. B*, **41** (2010), 670.
20) S. R. Chang, J. M. Kim and C. P. Hong: *ISIJ Int.*, **41** (2001), 738.
21) S. P. Wu, D. R. Liu, J. J. Guo, C. Y. Li, Y. Q. Sun and H. Z. Fu: *Mater. Sci. Eng. A*, **42** (2006), 240.
22) A. Kumar, M. J. Walker, S. Sundarraj and P. Dutta: *Metall. Mater. Trans. B*, **42** (2011), 825.
23) A. Kumar, M. J. Walker, S. Sundarraj and P. Dutta: *Metall. Mater. Trans. B*, **42** (2011), 783.
24) Y. H. Yang, B. Song, Z. B. Yang, G. Y. Song, Z. Y. Cai and Z. C. Guo: *Materials*, **9** (2016), 1001.
25) X. L. Liao, Q. J. Zhai, J. Luo, W. J. Chen and Y. Y. Gong: *Acta Mater.*, **55** (2007), 3103.
26) Y. Y. Gong, J. Luo, J. X. Jing, Z. Q. Xia and Q. J. Zhai: *Mater. Sci. Eng. A*, **497** (2008), 147.
27) J. F. Löffler and W. L. Johnson: *Intermetallics*, **10** (2002), 1167.
28) M. Y. Wang, Z. Wang and Z. C. Guo: *Int. J. Hydrog. Energy*, **35** (2010), 3198.
29) Y. Watanabe and S. Oike: *Acta Mater.*, **53** (2005), 1631.
30) Y. Watanabe, Y. Hattori and H. Sato: *J. Mater. Process. Technol.*, **221** (2015), 197.
31) Y. Watanabe, N. Yamanaka and Y. Fukui: *Metall. Mater. Trans. A*, **30** (1999), 3253.
32) S. El-Hadad, H. Sato and Y. Watanabe: *J. Mater. Process. Technol.*, **210** (2010), 2245.
33) S. El-Hadad, H. Sato, E. Miura-Fujiwara and Y. Watanabe: *Materials*, **3** (2010), 4639.
34) F. Kohler, L. Germond, J. D. Wagnière and M. Rappaz: *Acta Mater.*, **57** (2009), 56.
35) M. C. Flemings: *ISIJ Int.*, **40** (2000), 833.
36) Y. Watanabe, Y. Inaguma, H. Sato and E. Miura-Fujiwara: *Materials*, **2** (2009), 2510.
37) Y. Watanabe, A. Kawamoto and K. Matsuda: *Compos. Sci. Technol.*, **62** (2002), 881.
38) M. J. Assael, A. E. Kalyva, K. D. Antoniadis, B. R. Michael, I. Egry, J. T. Wu, E. Kaschnitzet and W. A. Wakeham: *J. Phys. Chem. Ref. Data*, **39** (2010), 33105.
39) P. Terzieff: *J. Alloy. Compd.*, **473** (2009), 195.
40) J. Kestin, M. Sokolov and W. A. Wakeham: *J. Phys. Chem. Ref. Data*, **7** (1978), 941.
41) J. S. McNown and J. Malaika: *Eos Trans. AGU*, **31** (1950), 74.
42) M. C. Flemings: *Metall. Trans. B*, **22** (1991), 269.
43) K. Kocatepe and C. F. Burdett: *J. Mater. Sci.*, **35** (2000), 3327.
44) F. Taghavi, H. Saghafian and Y. H. K. Kharrazi: *Mater. Des.*, **30** (2009), 115.
45) F. Taghavi, H. Saghafian and Y. H. K. Kharrazi: *Mater. Des.*, **30** (2009), 1604.
46) N. Iqbal, N. H. van Dijk, S. E. Offerman, M. P. Moret, L. Katgerman and G. J. Kearley: *Acta Mater.*, **53** (2005), 2875.
47) H. Men and Z. Fan: *Acta Mater.*, **59** (2011), 2704.
48) M. Easton and D. Stjohn: *Metall. Mater. Trans. A*, **6** (1999), 1613.
49) H. S. Jiang, M. Y. Zheng, X. G. Qiao, K. Wu, Q. Y. Peng, S. H. Yang, Y. H. Yuan and J. H. Luo: *Mater. Sci. Eng. A*, **684** (2017), 158.
50) B. Pourbahari, H. Mirzadeh and M. Emamy: *Mater. Sci. Eng. A*, **680** (2017), 39.